Phototriggered Linkage Isomerization in Ruthenium−Dimethylsulfoxyde Complexes: Insights from Theory

Ilaria Ciofini,[†] Claude A. Daul,[‡] and Carlo Adamo*[,†]

Laboratoire d'Electrochimie et Chimie Analytique, UMR CNRS-ENSCP no. 7575, Ecole Nationale Supérieure de Chimie de Paris, 11 rue P. et M. Curie, F-75231 Paris Cedex 05, France, and Departement de Chimie, Université de Fribourg, CH-1700, Pérolles Fribourg, Switzerland

Received: June 16, 2003; In Final Form: September 29, 2003

The ground and excited-state properties of $[Ru(bpy)(tpy)dmso]^{2+}$ (bpy = 2,2′-bipyridine, tpy = 2,2′:6′,2″-terpyridine; dmso = dimethyl sulfoxide) have been studied by the means of density functional theory (DFT). In particular, the singlet ground state and the potential energy surface of the lowest triplet were investigated along the coordinate involved in the S → O linkage isomerization of dmso. The time-dependent-DFT approach (TDDFT) was used to interpret the absorption spectra of the system, while a ΔSCF procedure was applied to compute the emission spectra. The good agreement between computed and experimental spectra highlights the power of DFT approaches in the description of complex transition metal containing systems. In addition, this method allows the full description of the ground and excited potential energy surfaces of $[Ru(bpy)(tpy)dmso]^{2+}$ which can only be roughly derived from experimental data, thus providing clues for further improvement in the engineering of phototriggering materials.

1. Introduction

Complexes of Ru(II) with polypyridine ligands (such as py, bpy, or tpy; py = pyridine, bpy = 2,2′-bipyridine, tpy = 2,2′:6′,2″-terpyridine) have been deeply studied from an experimental point of view[1−5] since their potential industrial applications, ranging from photovoltaic[6−9] (as component in solar energy batteries) to light switches[10−13] to biochemistry (as, for instance, DNA binding[14−17]) attracted chemists' interest. Even though the peculiar photochemical properties of the parent complex $[Ru(bpy)_3]^{2+}$ were discovered almost 30 years ago,[18] a strong and vital effort is still going on in order to enhance the properties of these systems via different functionalizations of the polypirydil ligands or their derivatives with different molecules (such as, for instance, cyanide,[19] thiocyanide,[20] dimethyl sulfoxide,[21] and sulfoxide[22]).

Within the large class of Ru−polypyridyl complexes, recently $[Ru(bpy)(tpy)dmso](SO_3CF_3)_2$ (dmso = dimethyl sulfoxide, see Figure 1) was synthesized and characterized.[23] This system is particularly interesting since all the photochemical properties of the Ru(II) center are coupled with the possibility of a S−O linkage isomerization of dimethyl sulfoxide, thus adding a tunable degree of freedom to the already remarkable properties of such class of complexes. Starting from the S linked isomer (in film or crystal), Rack and co-workers[23] showed that, after irradiation at 441.6 nm, an immediate change in color from yellow to red, associated with an absorption shift from 412 to 490 nm, is observed. Furthermore, the corresponding photoproduct is stable for days. The same complex is luminescent (upon irradiation at 441.6 nm) at 720 nm and, upon cooling, also at 625 nm.[23]

These experimental observations lead to the conclusion that the absorption at 412 nm is related to the transition from the singlet ground state (S_0) to the first singlet excited state (S_1) of the S-linked form. Irradiation then induces S−O linkage isomerization and the new feature appearing at 490 nm is due to the same $S_0 \rightarrow S_1$ transition as for the O-linked species. The photoproduct can be directly converted to the original S-linked species material only in dmso and in other coordinating solvents (i.e., CH_3CN) where it undergoes to an exchange of the ligand with a solvent molecule.[23] The emission at 720 nm is assigned to a triplet to singlet decay ($T_1 \rightarrow S_0$) of the O-linked species, while the band at 625 nm is assigned to a similar $T_1 \rightarrow S_0$ transition of a hypothetical η^2 species, characterized by a SO-metal bond.[23]

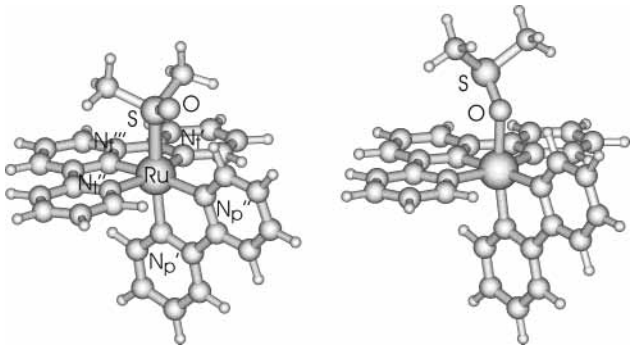

Figure 1. Schematic sketch and labeling scheme for the S-linked (left) and O-linked (right) isomers of $[Ru(bpy)(tpy)dmso]^{2+}$.

Both the S-linked and the O-linked isomers have been previously characterized. In particular, the synthesis and absorption spectra of the S-linked $[Ru(bpy)(tpy)dmso]^{2+}$ was reported by Root and Deutsch as product of the oxidation of $[Ru(bpy)(tpy)S(CH_3)_2]^{2+}$ with H_2O_2.[24] On the other hand, Roeker and co-workers synthesized the O-linked form in CH_3CN solution by addition of $S(CH_3)_2$ to $[Ru(tpy)(bpy)O]^{2+}$.[25] In none of these studies, all carried out in solution, were evidences of S−O (or O−S) linkage isomerization found. However, a substitution

* Corresponding author. E-mail: adamo@ext.jussieu.fr.
† ENSCP.
‡ University of Fribourg.

10.1021/jp0307607 CCC: $25.00
Published on Web 11/21/2003

reaction with the solvent (CH_3CN) was observed.[25] Roeker and co-workers[25] reported evidence of S−O linkage isomerization when using $[Ru(bpy)_2py(dmso)]^{2+}$ in CH_3CN solution, but the reaction finally lead to substitution of dmso by the solvent.

All these evidences support the hypothesis that the barrier for S−O linkage isomerization for the ground state of $[Ru(bpy)(tpy)(dmso)]^{2+}$ is rather large: i.e., not accessible at room temperature. Therefore, the linkage isomerization necessarily involves the population of an excited state, either with a metal to ligand charge transfer (MLCT) or a ligand field (LF) state. At the same time, the experimental data suggest that the linkage isomerization, contrary to similar Ru−dmso complexes such as $[Ru(bpy)_2(dmso)_2]^{2+}$,[21] is an intramolecular process in film and in the solid state, where the dmso ligand never leaves the coordination sphere of the metal atom.[23] Therefore, the linkage isomerization of dmso in $[Ru(bpy)(tpy)dmso]^{2+}$ is an unique case, and it can be considered as an extremely intriguing system for photoactive materials due to the possibility of switching the absorption spectra of the systems via functionalization.

The overall process seems to be well characterized at the experimental level, but the details are still lacking. In particular, while the overall assignment of the absorption spectra is out of query, the actual shape of the potential energy surface and the real nature of the emitting states at 625 and 720 nm are based on a more speculative basis.[23]

In such circumstances, insights from theoretical methods can be extremely useful to better understand the nature of both the ground and the excited states of $[Ru(bpy)(tpy)dmso]^{2+}$ as well as the actual mechanism of the photoisomerization. To correctly describe these phenomena, we need a theoretical method able to describe with comparable accuracy and, possibly, limited cost (due to the size of the system) both the ground and the excited potential energy surfaces as well as vertical excitations.

Density functional theory (DFT) has been remarkably successful to evaluate a variety of ground-state properties of large complexes containing transition metal with high accuracy.[26−28] More recently, several papers have shown the potentiality of the time-dependent DFT approach (TDDFT) in the calculation of vertical electronic excitation spectra.[29−33] Despite this fact, very little theoretical work is available on ruthenium(II) polypyridyl complexes,[34−41] the limiting factor being the size of the system under investigation, especially where it concerns TDDFT calculations.[42−43] On the other hand, several ground linkage isomerization reactions, already subject to intense experimental studies,[44−47] have been recently successfully studied at the DFT level.[48−51]

In this paper, the combined use of DFT for the study of the ground-state singlet and triplet potential energy profiles and of TDDFT for the prediction of the absorption/emission spectra, was chosen as a reliable theoretical tool to investigate the properties of $[Ru(bpy)(tpy)dmso]^{2+}$.

The aim of this paper is to gain information on the physicochemical characteristics of the ground and low-lying excited states and, in particular, to investigate the shape of the S_0, T_1, and S_1 potential energies surface governing the isomerization reactions. At the same time, we want to understand the effective role played by the hypothetical SO linked species in such a reaction.

The paper is organized as follows. First, the geometrical and electronic structures for the singlet ground state and triplet excited state of the S- and O-linked forms are discussed. Next, the potential energy profile along the S−O linkage isomerization coordinate is analyzed both for the singlet and the triplet states, and finally, the absorption and emission spectra are reported and discussed in comparison with the experimental data.

2. Technical Details

All calculations were performed using the Gaussian98 program package.[52] The Becke three parameters hybrid exchange[53] and the Lee−Yang−Parr correlation[54] functionals (B3LYP) were used. A double-ζ quality LANL2DZ basis[55,56] was used for all atom but oxygen and sulfur which were described by a split valence Pople basis plus one polarization function (6-31G*[57]). The 28 inner core electrons of Ru(II) were described by the corresponding scalar relativistic electron core potential (ECP).[56] Such a level of theory (B3LYP + LANL2DZ basis set) has been successfully applied in a number of papers concerning the structure, spectroscopic properties, and reactivity of organometallic systems.[42,43,49]

When not differently specified, the structural optimizations were performed without symmetry constraints. The stationary points found on the PES were characterized by subsequent frequency calculations.

Absorption spectra were computed as vertical excitations from the minima of the S_0 PES using the TDDFT approach as implemented in Gaussian using the basis set previously described.[58] Emissions from the triplet states were computed as vertical decay using the ΔSCF procedure; i.e., the singlet energy was computed at the triplet geometry. In a previous work, we have showed that TDDFT and ΔSCF computations provide very close results (difference < 0.1 eV) as concerns excitations to and from the triplet state of related Ru compounds.[43]

All calculations of the triplet states were performed within a spin-unrestricted formalism and spin contamination, monitored by the expectation value of $\mathbf{S}^2$, was found to be negligible.

Finally, the electronic structure of these molecules has been investigated using the natural bond orbital (NBO) approach and the related natural population analysis (NPA).[59] The NPA approach is particularly effective for inorganic complexes, since it gives a description of the electronic distribution which is less sensitive to the computational parameters (e.g., basis set).[60]

3. Results

Ground (S_0) and Excited (T_1) State Isomers: S vs O Linked. The main geometrical parameters obtained from the structural optimization of the S_0 and T_1 states of $[Ru(tpy)(bpy)dmso]^{2+}$ are collected in Table 1 and compared with the available experimental data.[23] The labeling scheme is reported in Figure 1. Let us to start from the ground state of the S-linked isomer. In $[Ru(tpy)(bpy)dmso]^{2+}$ the rotation of the dmso moiety around the M−S (or M−O) bond adds some extra flexibility to the other internal degrees of freedom. Since an accurate investigation of the ground-state energy surface is mandatory in order to obtain reliable vertical electronic transitions to the excited states, as first step we have studied such "floppy" motion. Three different conformers have been localized, corresponding to all the possible orientations schematically depicted in Figure 2 (and labeled **1**, **2**, and **3**). Structures **1** and **3** were fully optimized in C_s symmetry, while structure **2** results from a calculation performed without symmetry constraints: all have been characterized by computing harmonic frequencies. The latter one (**2**) was found to be the lowest in energy, 0.4 and 3.0 kcal/mol more stable than structure **1** and structure **3,** respectively. In the two extreme structures (**1** and **3**) the N_p−Ru−S−O dihedral angles correspond to values of 0 and 180°, while the angle is −31° for the most stable conformers (see Table 1 and Figure 2).

TABLE 1: Main Geometrical Parameters (Å and deg) for All Possible Isomers of the [Ru(bpy)(tpy)dmso]$^{2+}$ Complex, either in the Ground Singlet (S_0) or in the First Triplet (T_1) State[a]

	S_0				T_1
S-linked	**1**	**3**	**2**	exptl[b]	**7**
Ru−S	2.440	2.443	2.419	2.282	2.509
S−O	1.504	1.502	1.505	1.467	1.504
Ru−N'_t	2.116	2.120	2.113	2.079	2.099
Ru−N''_t	2.007	2.010	2.007	1.975	2.035
Ru−N'''_t	2.116	2.120	2.113	2.072	2.098
Ru−N''_p	2.142	2.136	2.142	2.101	2.122
Ru−N'_p	2.103	2.092	2.103	2.085	2.089
a(O−S−Ru)	117.1	112.6	114.5	115.7	114.2
d(N_{pcis}-Ru−S−O)	0.0	180.0	−31.0	−42.6	−8.0

	S_0		T_1
O-linked	**4**	**5**	**8**
Ru−O	2.195	2.192	2.102
S−O	1.564	1.564	1.591
Ru−N'_t	2.106	2.104	2.087
Ru−N''_t	2.000	2.000	2.008
Ru−N'''_t	2.106	2.109	2.112
Ru−N''_p	2.098	2.098	2.117
Ru−N'_p	2.065	2.065	2.071
a(S−O−Ru)	127.0	126.5	124.3
d(N_{pcis}-Ru−S−O)	0.0	−21.0	154.1

	S_0	T_1
SO-linked	**6**	**9**
Ru−O	3.156	2.949
RuS	3.089	3.094
S−O	1.526	1.518
Ru−N'_t	2.113	2.115
Ru−N''_t	2.008	2.023
Ru−N'''_t	2.107	2.116
Ru−N''_p	2.113	2.175
Ru−N'_p	2.029	2.138
a(S−O−Ru)	73.4	80.2
d(N_{pcis}-Ru−S−O)	−36.0	−4.4

[a] cis = cis with respect to dmso. N_t = nitrogen of tpy; N_p = nitrogen of bpy. [b] Ref 23.

Because of the small energy difference found for the three conformers, it could be argued that dmso is practically free to rotate at room temperature. To further elucidate this point we have performed some linear synchronous transit computations to estimate the interconversion barriers. We have found a relatively small activation energy for the **2** → **1** conversion (about 6 kcal/mol), while a higher barrier (about 40 kcal/mol) has been computed for the rotation from structure **2** to structure **3**. This last result is related to the steric interaction between hydrogens of dmso with the hydrogen of the bpy ligand when the N_p−Ru−S−O angle is around 140°. Because of this barrier, we can safely assume that the vertical excitations recorded in the absorption spectra for the S-linked S_0 will arise only from structure **2** and, eventually, structure **1**, and therefore, only these structures will be considered in the following.

As concerns all the other geometrical parameters, those related to the structure **2** are indeed the most similar to the X-ray structure, with an overall satisfactory agreement between the theoretical and the experimental data, all the computed distances being within the experimental error (±0.03 Å). This accuracy is the one expected for the used method, taking also into account experimental factors (e.g., crystal packing forces) which occasionally can be responsible for apparent discrepancies as for the Ru−S distance, overestimated by 0.13 Å. These results are in line with the errors found for similar systems at the same level of theory. Even a larger basis set, including polarization functions, does not appreciably improve the computed structures.[49,42]

TABLE 2: Natural Population Analysis for Ground (S_0) and First Triplet States (T_1) of All Three Isomers of the [Ru(bpy)(tpy)dmso]$^{2+}$ Complex

	S-linked		O-linked		SO-linked	
atom/	S_0	T_1	S_0	T_1	S_0	T_1
fragment	**2**	**7**	**5**	**8**	**6**	**9**
Ru	0.464	0.840	0.717	1.045	0.720	0.976
S	1.401	1.378	1.208	1.203	1.190	1.170
O	−0.944	−0.936	−0.940	−0.905	−0.982	−0.968
bpy	0.460	0.644	0.430	0.290	0.512	0.370
tpy	0.686	0.305	0.631	0.357	0.648	0.582
dmso[a]	0.390	0.211	0.222	0.308	0.119	0.072

[a] Bare dmso: $q(S) = 1.212$; $q(O) = -0.961$.

The vibrational analysis for the three minima confirmed their nature, all frequencies being positive. In Figure 3, we report the calculated infrared (IR) spectra for the S-linked species. Among all the transitions, the SO stretching frequency, the fingerprint transition for the investigated isomers, of the structure **2** was computed at 1118 cm^{-1}, in good agreement with the experimental findings (1102 cm^{-1}).[24] Nevertheless, the computed SO stretching frequency is not strongly affected by the rotation of dmso (max. variation 5 cm^{-1}): thus, it cannot be used as a screening criterion to understand the conformation of dmso. It is noteworthy to underline the difference between the computed frequency in the complex and in the bare dmso (ν(SO) = 1104 cm^{-1}). This difference can easily be related to the increase of the SO bond strength when going from the free to the complexed ligand, thus reflecting the difference found for the computed bond lengths when going from the free to the complexed dmso (+0.06 Å). A possible explanation of the SO shortening and increase of the ν(SO) when going from free dmso to the complex (observed also for other S-linked sulfoxide complexes of Ru(II)[24]) can be that upon complex formation the polarization of the SO bond increases due to electron depletion as a consequence of the π S−Ru donation.

Better insights on the electronic structures of such complexes can be obtained by looking at the NPA charges, reported in Table 2. These charges well underline the trends found in the geometrical and spectroscopical parameters. In fact, if we take as references the two fragment, [Ru(bpy)(tpy)]$^{2+}$ and dmso, the charge transferred to the metallic moiety is 0.39 |e$^-$|, mainly due a depletion of the sulfur atom, the charge on S being 1.40 |e$^-$| in the complex and 1.21 |e$^-$| in the bare dmso. These values point out a relatively strong donation from dmso to Ru, which is only partially compensated for by the corresponding back-donation. This latter mechanism is unlike because of the steric constraints which do not allow for an adequate d−π* overlap. It is also interesting to note the relatively small positive charges localized on the metal atom, which is far from its formal +2 oxidation state (+0.46 |e$^-$|).

Frontier orbitals play a relevant role in such systems, since they determine the spectroscopic behavior of such complexes. Here, the analysis of the molecular orbitals for the complex **2** reveals the typical features of octahedral coordinated Ru(II)-polypyridil complexes (such as Ru(bpy)$_3^{2+}$[40] or Ru(bpy)$_2$CN$_2$[43]) where the highest occupied molecular orbital (HOMO) has mainly d metallic character while the lowest unoccupied molecular orbital (LUMO) is essentially a π* orbital localized on the bipyrdil ligand, thus all the active transitions to this last orbital can be described as metal to ligand charge transfer

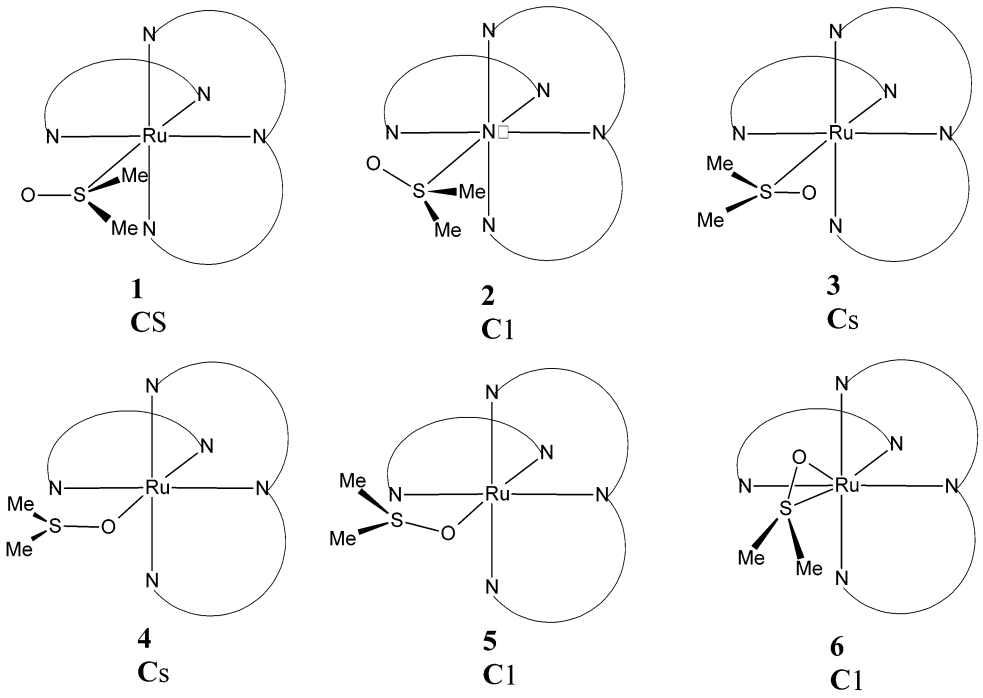

Figure 2. Different orientations of the dimethyl sulfoxide ligand in the localized conformers of S-linked (up) and O-linked (down) complexes and relative labeling and symmetry.

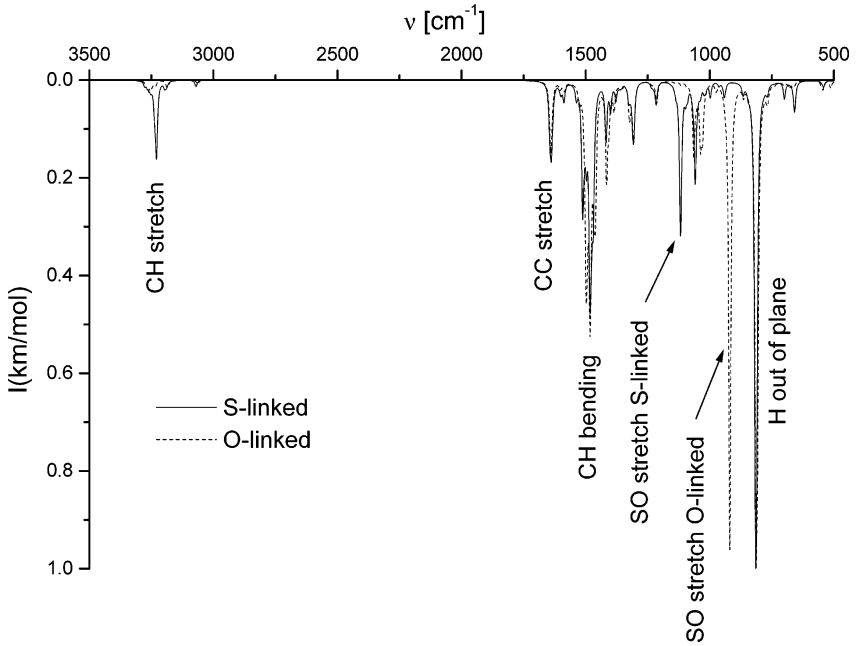

Figure 3. Theoretical IR spectra for the S-linked and O-linked isomers. The spectra are reproduced by associating a single Lorentzian function to each computed transition, with half-height width of 10 cm^{-1}. Intensities are normalized to 1.

(MLCT) bands (vide infra). An isovalue representation of such frontier orbitals of **2** is reported in Figure 4.

In the case of the O-linked S_0 state, two different minima were characterized in the ground state: one with a 0° $N_p-Ru-O-S$ dihedral angle (C_s symmetry, **4** in Figure 2) and one with a −21° $N_p-Ru-O-S$ dihedral angle (C_i, **5** in Figure 2). Even though in this case a structure corresponding to $d(N_p-Ru-O-S) = 180°$ is likely to exist, we do not attempt to localize it, since, as for the S-linked case, it should lie quite high in energy and should not be accessible at room temperature. The non-symmetric conformation (**5**) was found to be practically isoenergetic (energy difference < 0.1 kcal/mol) with respect to the one with C_s symmetry (**4**). Thus, the UV−vis transitions were computed both for **4** and **5**.

Surprisingly, the O-linked conformer (**5**) lies 11 kcal/mol lower in energy that the corresponding S-linked one (**2**, see Table 3). These data seem contradictory to the experiment where only the S-bound form has been crystallized.[23] Nevertheless, the main reason for formation of the S-linked isomer is most probably kinetic and not thermodynamic. In fact, a smaller volume computed for the S-linked molecules with respect to the O linked one (3754 $bohr^3$/mol vs 3785 $bohr^3$/mol) justifies the preferential crystallization observed since a better packing is possible. Nevertheless, since the computed differences in

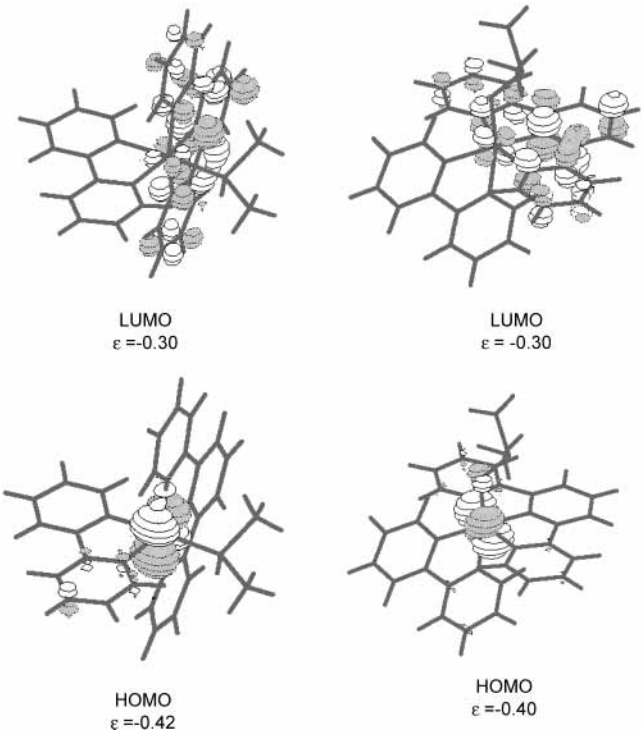

Figure 4. Plot of isodensity surfaces (contour value $\pm 0.05(e/Å^3)^{1/2}$) for the highest occupied and lowest unoccupied molecular orbitals of the S-linked (left) and O-linked isomers (right). The MO energy (ϵ) is reported in hartrees.

TABLE 3: Relative Energies (eV) for the Electronic States of All Considered Complexes[a]

		T_1		S_1
	S_0	ΔSCF	TDDFT	TDDFT
S-linked	0.0	2.20 (2.12)	2.26	3.08
SO-linked	0.60	2.32 (2.23)		
O-linked	−0.05	1.83 (1.75)	1.90	2.78

[a] All of the values have been computed using the ground state optimized geometries, except for the values reported in parentheses, which have been carried out using optimized triplet geometries.

energy and in volume are rather small, we cannot rule out the role stabilizing one of the two conformers.

As before, both structures were characterized, by computing harmonic frequencies. In particular, the SO stretching vibration is found at 919 cm^{-1} for the minimal energy structure (**5**), lower that the corresponding S-linked form (**2**) (1118 cm^{-1}). The plot of Figure 3 displayed quite well the fingerprint regions of the two isomers. This result is in agreement with the experimental observations for a number O-linked sulfoxide Ru(II) complexes, where the SO stretch is recorded in the range 900−935 cm^{-1}.[25] At the same time, the smaller wavenumber reflects the increasing d−π* back-bonding character of the O-linked dmso with respect to the S-linked isomer. In fact**,** comparing the S_0 structures for the S linked (**2**) and O-linked form (**5**), we can notice an elongation of the S−O bond going from the S- to the O-linked one (0.06 Å). The elongation can be related to the better back-bonding character of the dmso O-linked with respect to the S-linked conformation: the S atom acts mainly as a σ donor when coordinating while the O atoms can act as σ,π donor and π* acceptor as well. As a consequence, as soon as the Ru−O bond is strengthened due to stronger $\sigma\pi$ interactions, the SO bond is lengthened due to d−π* back-bonding. Furthermore, the S−O−Ru angle gets larger with respect to the O−S−Ru of the S linked form (+14°) tending toward a linear S−O−Ru conformation in order to maximize Ru−O π interactions. Thus, the HOMO gets significant contributions from the p orbital of O, still remaining mainly d Ru centered (see Figure 4).

The larger back-bonding interaction is further confirmed by the NPA charge analysis: when going from the S-linked (**2**) to the O-linked (**5**) conformers the charge on Ru increases from 0.46 to 0.72 $|e^-|$ while that on O remains constant (about −0.94 $|e^-|$). At the same time, a decrease of the positive charge localized on sulfur is found (from 1.40 to 1.21 $|e^-|$, where 1.21 $|e^-|$ corresponds to the free dmso). The overall effect is a decrease of the positive charge on the dmso in going from the S-linked to the O-linked isomer (from 0.39 to 0.22 $|e^-|$). So, while dmso in the S-linked species acts as a good σ donor and poor π acceptor, it becomes (mainly due to the more flexible conformation) a good π acceptor in the O-linked isomer. This behavior has already been suggested by experimentalists in relationship with the spectral shift to higher energy observed in going from the O-linked to the S-linked species.[24,59] It is also interesting to note the overall electronic rearrangement in this latter isomer, characterized by a decrease of the positive charges localized on the bpy and tpy ligands. In particular, the ruthenium atom can be considered as a Ru(I), with the other positive charge delocalized on the aromatic rings. This behavior has been reported for other Ru(II) complexes with good donor ligands (such as CN or SCN).[43]

The lowest triplet state, T_1, has been analyzed by carrying out unrestricted calculations, both at the corresponding S_0 geometries and at the fully optimized triplet structures. The calculated energy gaps with respect to the ground electronic state are reported in Table 3. They have been computed both as energy difference with respect to S_0 (the so-called ΔSCF approach) as well as by the TDDFT approach. In all the considered complexes, the triplet state corresponds to an excitation from the HOMO to the LUMO (see Figure 4).

The optimized T_1 state for the S-linked isomer lies 2.1 eV higher than the corresponding ground state. The corresponding optimized structure, labeled **7** in Table 1, was obtained starting from the optimized singlet structure **2** (no symmetry constraints imposed) and has been characterized as a minimum by frequency computations. By comparison with the S_0 structure a significant elongation of the Ru−S bond (+0.09 Å) and smaller contraction of the Ru−N_t and Ru−N_p bonds can be noticed, while the internal dmso parameters are not significantly affected. A slight rotation (+23°) of dmso toward a C_s orientation can also be remarked. In general, the variation of the geometrical parameters is in line with the nature of the transition. In fact the $S_0 \rightarrow T_1$ transition formally corresponds to a transfer of one electron from the HOMO (Ru d_π orbital, slightly antibonding with bpy) to a MO with mainly π* tpy contribution and a smaller Ru−dmso antibonding character (see Figure 4). Since an electron has been removed from a Ru−L antibonding orbital (L = bpy,tpy), the main structural consequence to be expected is a contraction on Ru−N_t and Ru−N_p lengths as indeed observed. This is qualitatively confirmed by the corresponding TDDFT calculations (vide infra) and by the computed Mulliken spin population of the optimized S-linked T_1 state: 0.9 on Ru and 1.0 on tpy ligand. It also interesting to note either the small energy difference between the results obtained with optimized and those using frozen geometries. At the same time TDDFT and ΔSCF computations show close results, thus pointing out the one-electron nature of these excitations (see Table 3).

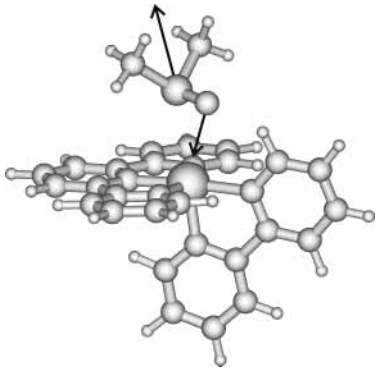

Figure 5. Structure of the transition state for the S-linked → O-linked interconversion in the ground state (S_0). The arrows on the picture indicate the different components of the transition vector (ν = 157i cm^{-1}).

The structural optimization of the O-linked triplet state ($^3T_1$), starting from the optimized S_0 O-linked structure (**5**), lead to two different minima, the first one being less stable than the second (difference in energy of about 2 kcal/mol). The structure **8** corresponds to the minimum for the $^3T_1$ state and it is characterized by a shorter Ru−O distance (2.10 Å) and a longer SO length (1.59 Å, see Table 1). The two variations suggest an increase of the dmso−metal interactions (donation and back-donations), due to the depletion of the HOMO orbital, with a significant Ru−O antibonding contribution, upon excitation. All the other geometrical parameters are less affected by the transition. As for the S-linked isomer, there is an overall coherence in the results obtained with frozen and relaxed structures with TDDFT or ΔSCF approaches (see Table 3).

The other characterized structure (C_s symmetry, values not reported in Table 3), even if high in energy, is noteworthy. In fact it corresponds to an $S_0 \rightarrow T_1$ ligand field (LF) transition, as confirmed by the computed Mulliken spin density on Ru (1.84 e^-). This state is practically dissociative for dmso as the longer Ru−O distance suggests (about 2.55 Å). Since this state is only slightly higher in energy, it could be populated in particular chemical conditions (e.g., in solution) and be responsible for the exchange mechanism experimentally observed.[23]

Ground (S_0) and Excited (T_1) State S—O Linkage Isomerization Profile. As mentioned in the Introduction, a η^2 species has been proposed as intermediate along the linkage S → 0 isomerization path, to explain the peculiar spectroscopic behavior.[23] For this reason, a transition state (TS) search was performed both on the S_0 and on the T_1 potential energy surfaces. With this procedure, a first-order transition state (ν = 157i cm^{-1}) was localized on the S_0 surface and characterized by a imaginary frequency corresponding to the isomerization path. In Figure 5, we have reported the optimized structure of this TS, together with the transition vector components. As it appears from this sketch, the structure can be described as a heptacoordinate rearrangement, with the dmso in the supposed η^2 coordination. Such a rearrangement has been found for other linkage isomerization (see for instance ref 48). This structure (labeled **6** in Table 1) lies 13.9 kcal/mol higher than the S-linked structure (**2**) and 25.6 kcal/mol higher than the O-linked one (**5**). Its main geometrical parameters are reported in Table 1. The geometrical parameters indicate that the S and the O atoms of dmso are at almost the same, relatively large, distance from the Ru atom (3.09 vs 3.16 Å, respectively). At the same time, the internal geometrical parameters of the dmso are close to those of the free ligand. For instance, the SO length is 1.53 in the complex and 1.51 Å in the bare molecule. The NPA charges (reported in Table 2) also indicate a decreases of the Ru−dmso interaction. In fact the dmso fragment has an overall charge of +0.12 $|e^-|$, thus suggesting that less electron density is transferred to the Ru complex than in the two minima. At the same time the computed interaction energy of the dmso with $[Ru(bpy)(tpy)]^{2+}$ is 17.4 kcal/mol, significantly lower than in the S-linked (30.3 kcal/mol) or in the O-linked (42.1 kacl/mol) isomer.

The structures of the reactants and of the TS allow for the evaluation of a significant thermodynamic activation parameters, namely the activation volume. This quantity is certainly interesting in defining the nature of a substitution reaction, i.e., if the mechanism is dissociative (D) associative (A) intermediate associative (I_a) or intermediate dissociative (I_d). In this isomerization, both A and D mechanisms are ruled out in the film or solid state, where a intermediate reaction has been suggested,[23] while a dissociative process is most probable in dmso solution.[24] To have an estimation of the activation volumes for the different species, we evaluate the sum of the metal to dmso distances, which is directly proportional to such volumes. This approach has already been applied in the literature for other substitution reactions (see for instance refs 49 and 61). The activation volume is therefore proportional to Σ, the difference between the TS and the S-linked or volumes, estimated as

$$\Sigma = \sum_i d(\mathrm{Ru-X}_i)_{\mathrm{TS}} - d(\mathrm{Ru-X}_i)_{\mathrm{S-linked}}$$

where X represents the coordinating atoms of dmso. From the computed structure, we found a value of +0.31 Å. A small positive value suggests a slight preference for the I_d or D reaction, at least in the isolated molecule. So, the nature of the TS explains why such reactions are likely to occur in solution.

Starting from the TS localized on the S_0 surface the corresponding intermediate structure has been localized on the T_1 surface. This structure is characterized by one imaginary frequency (ν = 101i cm^{-1}) and is about 3.0 kcal/mol higher than the S isomer and 13.1 kcal/mol with respect to the O-linked form (see Table 3). The small barrier for S → O interconversion (3.0 kcal/mol) demonstrates quite well the possibility of an isomerization in the T_1 state, going through a direct, single-step reaction. These results invalidate the two-step mechanism supposed by the experimentalists, where the SO η^2 structure is a minimum on the T_1 surface and where two energy barriers have to be overcome for the complete isomerization.[23] This mechanism has been proposed on the basis of the band at 625 nm in the emission spectrum, which was assigned to such an η^2 intermediate. Our calculations show, instead, that the diabatic emission of the TS, i.e., a hypothetical decay to the corresponding TS on the S_0 surface, is at 761 nm (1.7 eV), far from the observed transition. The adiabatic transition of the TS is, of course, at an even lower energy. The observed transition can be assigned, instead, to the decay of the triplet state of the S-bonded isomer (vide infra).

The calculated geometrical parameters of the TS are reported in Table 1. These values are similar to those computed for the TS of the ground state, the only appreciable differences concerning the Ru−O distance, shorter in the T_1 state, and the rotation angle of the dmso with respect to the bpy. The first variation is particularly important, since it suggests a more compact structure of the TS in the T_1 state, as also suggested by the greater interaction energy of the dmso with $[Ru(bpy)(tpy)]^{2+}$ fragment (21.3 kcal/mol). These latter values, together with a smaller value of Σ, +0.12 Å, strongly suggests that the

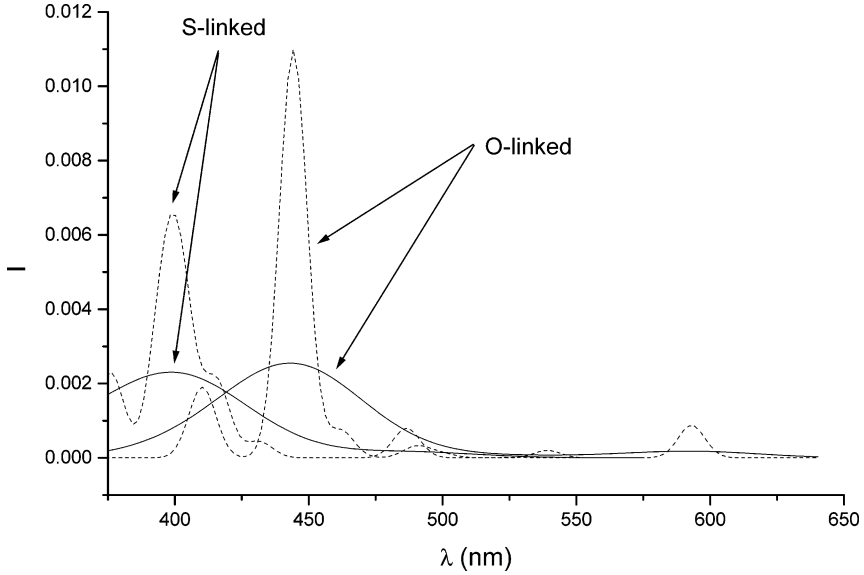

Figure 6. Computed UV spectra for the S- and O-linked isomers. The spectra are reproduced by associating a single Lorentzian function to each computed transition and normalizing the absorbance to 1. Full line plot corresponds to a broadening of 0.5 eV, dotted line plot to a broadening of 0.2 eV.

TABLE 4: Computed TDDFT Vertical Excitation Energies (λ, nm) and Oscillator Strengths (f) for the Most Stable S-linked Isomer, Where the Values in Parentheses Refer to the System in C_s Symmetry

transition	λ	f	orbital contributions	character[a]
$S_0 \rightarrow S_n$	486	0.0100	d $\rightarrow \pi^*$	MLCT
	(483)	(0.0100)		
	416	0.0260	d $\rightarrow \pi^*$	MLCT
	402	0.0541	d $\rightarrow \pi^*$	MLCT
	396	0.0481	d $\rightarrow \pi^*$	MLCT
	378	0.0027	d $\rightarrow \pi^*$	MLCT
	376	0.0267	d $\rightarrow \pi^*$	MLCT
	335	0.0016	d $\rightarrow \pi^*$	MLCT
$S_0 \rightarrow T_n$	547	0.0	d $\rightarrow \pi^*$	MLCT
	(545)			

[a] MLCT = metal to ligand charge-transfer band.

TABLE 5: Computed TDDFT Vertical Excitation Energies (λ, nm) and Oscillator Strengths (f) for the Most Stable O-linked Isomer, Where the Values in Parentheses Refer to the System in C_s Symmetry[a]

transition	λ	f	orbital contributions	character[a]
S_0-S_n	593	0.0110	d $\rightarrow \pi^*$	MLCT
	(596)	(0.0113)		
	490	0.0039	d $\rightarrow \pi^*$	MLCT
	462	0.0093	d $\rightarrow \pi^*$	MLCT
	445	0.0661	d $\rightarrow \pi^*$	MLCT
	444	0.0287	d $\rightarrow \pi^*$	MLCT
	443	0.0474	d $\rightarrow \pi^*$	MLCT
	410	0.0239	d $\rightarrow \pi^*$	MLCT
S_0-T_n	653	0.0	d $\rightarrow \pi^*$	MLCT
	(652)		d $\rightarrow$ d	LF

[a] MLCT = metal to ligand charge-transfer band; LF = ligand field band.

isomerization mechanism assume a more associative character (A or I_a) in the triplet state than in the ground singlet state.

In summary, our calculations suggest that the isomerization reaction is highly probable in the triplet state, due to the small barrier that can be easily overcome under experimental conditions. At the same time, the reaction mechanism is a single step, the transition structure corresponding to the SO η^2 arrangement.

Absorption and Luminescence. As the last step in our investigation of $[Ru(bpy)(tpy)dmso]^{2+}$, we have computed the UV spectra, on the minimal energy structures reported in Table 1, using a TDDFT approach. All these vertical electronic transitions have been evaluated at the corresponding ground-state geometries. The results are collected in Tables 4 and 5 for the S- and O-linked complexes, respectively. As mentioned in the Introduction, from experimental data collected both in films and in solution, the most intense MLCT transition occurs at 412 nm in the case of the S-linked complexes and it is shifted to 490 nm in the case of the O− linked one. As expected, both transitions are well described by the TDDFT approach, even if they are slightly overestimated. In particular, we have found three intense bands for the S-linked isomer, centered at 416, 402, and 396 nm. The corresponding bands for the O-linked species are at 462, 445, and 444 nm. All these transitions can be interpreted as one electron excitations from MOs centered on the d orbital of Ru(II) to empty π^* MOs localized on the tpy/bpy moieties, the transitions involving the bpy moieties occurring normally at higher energy. At the same time, several satellite transitions, either at higher or lower energies and with lower oscillator strengths, have been computed and all assigned to d $\rightarrow \pi^*$ excitations. From these results, it is clear that these most intense bands, rather broad, cover several transitions in the experimental spectra. A simulation of the spectra using different Lorenzian functions can easily illustrate this effect. Since the integral of the Lorenzian function is proportional to the oscillator strengths, the only adjustable parameters is the width at half-height, that is the broadening of the peak. The simulated spectra are reported in Figure 6. When the broadening of the line is around 0.5 eV or more, a single peak is detected, in agreement with the experimental data. In such circumstances, we can compare the energy of the experimental maxima with those of the simulated spectra and a good agreement is found in the case of the S-linked complex ($\Delta\lambda = 0.2$ eV) while a larger error ($\Delta\lambda = 0.5$ eV) is detected in the case of the O-linked system.

It is also interesting to note that our calculations also reproduce (even if not quantitatively) the red shift observed in going from the S-linked to the O-linked complex. This variation is consistent with the decrease of electron density on the metal resulting in a destabilization of its partially filled d orbitals, the

Ru bearing a larger positive charge in the O-linked than in the S-linked complex (see Table 2).

When neglecting spin−orbit coupling, as in our TDDFT computations, all singlet to triplet transitions are spin-forbidden, and as a consequence, the computed oscillator strength is zero and their intensity on the measured absorption spectra negligible. Nevertheless the vertical $S_0 \rightarrow T_1$ transition allows one to identify the character of the first excited triplet state. These first transitions have been computed using both a TDDFT and ΔSCF approach. In the first case, we find a transition at 547 and 653 nm for the S and O linked forms, respectively. For both the S- and O-linked isomers, the first $S_0 \rightarrow T_1$ transition involves mainly a MLCT transition. Nevertheless a substantial difference is found: while the S-linked triplet has a contribution only from MLCT transitions (essentially HOMO → LUMO), in the O-linked form a relatively small (10%) contribution arises from a ligand field (LF) transition. This corresponds to the promotion of an electron from a d_π orbital of Ru(II) to the d_{z^2} pointing toward the O atom of dmso. Therefore, when relaxing both the geometry and the electronic state of the T_1, we have found two minima (depending on the population of the LUMO or LUMO+8 orbital), one for each state. Emission is most probably occurring from the MLCT state since the T_1−LF state will lead to dissociation in solution.

While absorption spectra involve vertical transition from the ground (S_0) to the excited states, the emission spectra represent the vertical decay from the minima on the triplet potential energy surface (T_1) to the ground state (S_0). Therefore, to compute the emission spectra it is important to have a full description of the T_1 PES. Emissions from the S- and O-linked forms were computed using the ΔSCF procedure, using the relaxed T_1 geometries. We did not attempt to compute the emission spectrum using the TD-DFT approach since the use of this procedure to describe the triplet potential energy surfaces in the case of simple molecular systems, such as H_2,[62] or, more generally, in the case of transitions involving spin flips has been shown to give unphysical results.[63] The emission decay for the S-linked form was computed at 697 nm, rather close to the experimental value (625 nm) of the band occurring at low temperature.[23] This transition has been previously attributed to the decay of the SO intermediate, but this transition occurs at lower energy (761 nm). In the case of the O-linked form the emission decay was computed at 1130 nm for the LF state (**6**) while the $^3T_1$ MLCT state is predicted to emit at 744 nm. This latter value is in good agreement with the experimental finding (720 nm), thus confirming the nature of the first excited triplet state as a MLCT one.

4. Conclusions

We have given a full description of the ground and excited potential energy surfaces of $[Ru(bpy)(tpy)dmso]^{2+}$ using density functional theory. Our study focused on the spectrochemical properties of the complex (absorption and emission) along the S−O linkage isomerization coordinate. A good agreement between computed and experimental spectra was found for the S- and O− linked isomers. More interesting, our results showed that the η^2 SO-linked form, proposed to interpret the experimental emission data, does not correspond to a minimum on the potential energy surface either of the singlet ground state (S_0) or of the triplet first excited state (T_1). Instead, we found that the second observed emission band is likely to occur from the O-linked triplet.

More generally, our results highlight the power of DFT approaches in the description of complex transition metal containing systems especially helpful when the properties of the excited states can be only roughly derived from experimental data thus providing clues for further improvement in the engineering of phototriggering materials.

Acknowledgment. Prof. Henry Chermette (Lyon, France) is gratefully acknowledged for help in crystallographic search and helpful suggestions. I.C. and C.A. thank the CNRS for a financial support in the framework of the ACI "Jeune Equipe 2002" project. C.A.D. acknowledges the Swiss National Science Foundation for support.

References and Notes

(1) Juris, A.; Balzani, V.; Barigelletti, F.; Campagna, S.; Belser, P.; von Zelewsky, A. *Coord. Chem. Rev.* **1988**, *84*, 85.
(2) Kalyanasundaram, K. *Coord. Chem. Rev.* **1982**, *46*, 159.
(3) Balzani, V.; Juris, A.; Venturi, M.; Campagna, S.; Serroni, S. *Chem. Rev.* **1996**, *96*, 759.
(4) MacDonnel, F. M.; Kim, M. J.; Bodige, S. *Coord. Chem. Rev.* **1999**, *185*, 535.
(5) Krausz, E.; Riesen, H. *Coord. Chem. Rev.* **1997**, *159*, 9.
(6) Graetzel, M.; Reagan, B. O. *Nature (London)* **1991**, *353*, 737.
(7) Rudmann, H.; Shimada, S.; Rubner, M. F. *J. Am. Chem. Soc.* **2002**, *124*, 4918.
(8) Gao, F. G.; Bard, A. J. *J. Am. Chem. Soc.* **2000**, *122*, 7426.
(9) Cahen, D.; Grätzel, M.; Guillemoles, J. F.; Hodes, G. In *Electrochemistry of nanomaterials*; Hodes, G., Ed.; Wiley-VCH: New York, 2001.
(10) Olson, E. J. C.; Hu. D.; Hörmann, A.; Jonkman, A. M.; Arkin, M. R.; Stemp, E. D. A.; Barton, J. K.; Barbara, P. F. *J. Am. Chem. Soc.* **1997**, *119*, 11458.
(11) Stemp, E. D. A.; Barton, J. K.; Barbara, P. F. *J. Am. Chem. Soc.* **1997**, *119*, 2921.
(12) Marincola, F. C.; Casu, M.; Saba, G.; Lai, A.; Lincoln, P.; Nordén, B. *Chem. Phys.* **1998**, *236*, 301.
(13) Holmlin, R. E.; Stemp, E. D. A.; Barton, J. K. *Inorg. Chem.* **1998**, *37*, 29.
(14) Tuite, E.; Lincoln, P.; Nordén, B. *J. Am. Chem. Soc.* **1997**, *119*, 239.
(15) Zhen, Q. X.; Ye, B. H.; Liu, J. G.; Zhang, Q. L.; Ji, L. N.; Wang, L. *Inorg. Chim. Acta* **2000**, *303*, 141.
(16) Bhuiyan, A. A.; Kincaid, J. R. *Inorg. Chem.* **1999**, *38*, 4759.
(17) Bodige, S.; MacDonnel, F. M. *Tetrahedron Lett.* **1997**, *38*, 8159.
(18) Harrigan, R. W.; Crosby, G. A. *J. Chem. Phys.* **1973**, *59*, 3468.
(19) Nazeeruddin, M. K.; Kay, A.; Rodicio, I.; Humphry-Baker, R.; Muller, E.; Liska, P.; Vlachopoulos, N. Gratzel, M. *J. Am. Chem. Soc.* **1993**, *115*, 6382.
(20) Shklover, V.; Ovchinnikov, Y. E.; Braginsky, L. S.; Zakeeruddin, S. M.; Grätzel, M. *Chem. Mater.* **1998**, *10*, 2533.
(21) Smith, M.; K.; Gibson, J. A.; Young, C. G.; Broomhead, J. A.; Junk, P. C.; Keene, F. R. *Eur. J. Inorg. Chem.* **2000**, 1365.
(22) Kovalevsky, A.; Bagley, K.; Coppens, P. *J. Am. Chem. Soc.* **2002**, *124*, 9241.
(23) Rack, J. J.; Winkler, J. R.; Gray, H. B. *J. Am. Chem. Soc.* **2001**, *123*, 2432.
(24) Root, M. J.; Deutsch, E. *Inorg. Chem.* **1985**, *24*, 1464,.
(25) Roeker, L.; Dobson, J. C.; Vining, W. J.; Meyer, T. J. *Inorg. Chem.* **1987**, *26*, 779.
(26) Koch, W.; Holthausen, M. C. *A Chemist's Guide to Density Functional Theory*; Wiley-VCH: Weinheim, Germany, 2000.
(27) Adamo, C.; di Matteo, A.; Barone, V. *Adv. Quantum Chem.* **1999**, *36*, 4.
(28) Burke, K.; Perdew, J. P.; Wang, Y. In *Electronic density functional theory: recent progress and new derivations*; Dobson, J. F., Vignale, G., Das, M. P., Eds.; Plenum Press: New York, 1997.
(29) Boulet, P.; Chermette, H.; Daul, C. A.; Gilardoni, F.; Rogemond, F.; Weber, J.; Zuber, G. *J. Phys. Chem. A* **2001**, *105*, 885.
(30) Boulet, P.; Chermette, H.; Weber, J. *Inorg. Chem.* **2001**, *40*, 7032.
(31) Cavillot, V.; Champagne, B. *Chem. Phys. Lett.* **2002**, *354*, 449.
(32) Adamo, A. Barone, V. *Theor. Chem. Acc.* **2000**, *105*, 169.
(33) Farrell, I. R.; van Slageren, J.; Zalis, S.; Vlcek, A. *Inorg. Chim. Acta* **2001**, *315*, 44.
(34) Zheng, K.; Wang, J.; Shen, Y.; Peng, W.; Yun, F. *J. Comput. Chem.* **2002**, *23*, 436.
(35) Ziegler, M.; von Zelewsky, A. *Coord. Chem. Rev.* **1998**, *177*, 257.
(36) Broo, A.; Lincoln, P. *Inorg. Chem.* **1997**, *36*, 2544.
(37) Damrauer, N. H.; Boussie, T. R.; Deveney, M.; McCusker, J. K. *J. Am. Chem. Soc.* **1997**, *119*, 8253.
(38) Wakatsuki, Y.; Koga, N.; Yamazaki, H.; Morokumo, K. *J. Am. Chem. Soc.* **1994**, *116*, 8105.

(39) Zhang, L. T.; Ko, J.; Ondrechen, M. J. *J. Am. Chem. Soc*. **1987**, *109*, 166.
(40) Daul, C.; Baerends, E. J.; Vornooijs, P. *Inorg. Chem*. **1994**, *33*, 3538.
(41) Albano, G.; Belser, P.; Daul, C. A. *Inorg. Chem.* **2001**, *40*, 1408.
(42) Hay, P. J. *J. Phys. Chem. A* **2002**, *106*, 1634.
(43) Adamo, C.; Joubert, L.; Barone, V.; Guillemoles, J.-F *J. Phys. Chem. A* **2002**, *106*, 11354.
(44) Imlau, M.; Haussuhl, S.; Woike, T.; Schieder, R.; Angelov, V.; Rupp, R. A.; Schwarz, K. *Appl. Phys. B: Laser Opt.* **1999**, *68*, 877.
(45) Imlau, M.; Woike, T.; Schieder, R.; Rupp, R. A. *Phys. Rev. Lett.* **1999**, *82*, 2860.
(46) Woike, T.; Haussuhl, S.; Sugg, B.; Rupp, R. A.; Beckers, J.; Imlau, M.; Schieder, R. *Appl. Phys. B: Laser Opt.* **1996**, *63*, 243.
(47) Carducci, M. D.; Pressich, M. R.; Coppens, P. *J. Am. Chem. Soc.* **1997**, *119*, 2669.
(48) Schaiquevich, P. S.; Guida, J. A.; Aymonino, P. J. *Inorg. Chim. Acta* **2000**, *303*, 277.
(49) Ciofini, I.; Adamo, C. *J. Phys. Chem. A* **2001**, *105*, 1086.
(50) Boulet, P.; Buchs, M.; Chermette, H.; Daul, C. A.; Furet, E.; Gilardoni, F.; Rogemond, F.; Schläpfer, C. W.; Weber, J. *J. Phys. Chem. A* **2001**, *105*, 8999,.
(51) Boulet, P.; Buchs, M.; Chermette, H.; Daul, C. A.; Gilardoni, F.; Rogemond, F.; Schläpfer, C. W.; Weber *J. Phys. Chem. A* **2001**, *105*, 8991.
(52) Frisch, M. J.; Trucks, G. W.; Schlegel, H. B.; Scuseria, G. E.; Robb, M. A.; Cheeseman, J. R.; Zakrzewski, V. G.; Montgomery, J. A., Jr.; Stratmann, R. E.; Burant, J. C.; Dapprich, S.; Millam, J. M.; Daniels, A. D.; Kudin, K. N.; Strain, M. C.; Farkas, O.; Tomasi, J.; Barone, V.; Cossi, M.; Cammi, R.; Mennucci, B.; Pomelli, C.; Adamo, C.; Clifford, S.; Ochterski, J.; Petersson, G. A.; Ayala, P. Y.; Cui, Q.; Morokuma, K.; Malick, D. K.; Rabuck, A. D.; Raghavachari, K.; Foresman, J. B.; Cioslowski, J.; Ortiz, J. V.; Baboul, A. G.; Stefanov, B. B.; Liu, G.; Liashenko, A.; Piskorz, P.; Komaromi, I.; Gomperts, R.; Martin, R. L.; Fox, D. J.; Keith, T.; Al-Laham, M. A.; Peng, C. Y.; Nanayakkara, A.; Gonzalez, C.; Challacombe, M.; Gill, P. M. W.; Johnson, B.; Chen, W.; Wong, M. W.; Andres, J. L.; Gonzalez, C.; Head-Gordon, M.; Replogle; E. S.; Pople, J. A. *Gaussian 98*, Revision A.7; Gaussian, Inc.: Pittsburgh, PA, 1998.
(53) Becke, A. D. *J. Chem. Phys.* **1993**, *98*, 5648.
(54) Lee, C.; Yang, W.; Parr, R. G. *Phys. Rev. B* **1988**, *37*, 785.
(55) Dunning, T. H., Jr.; Hay, P. J. In *Modern Theoretical Chemistry*, Schaefer, H. F., III., Ed.; Plenum: New York, 1976; pp 1−28.
(56) Hay, J.; Wadt, W. R. *J. Chem. Phys.* **1985**, *82*, 299.
(57) Francl, M. M.; Petro, W. J.; Hehre, W. J.; Binkley, J. S.; Gordon, M.-H.; DeFree, D. J.; Pople, J. A. *J. Chem. Phys.* **1982**, *77*, 3654.
(58) Stratmann, R. E.; Scuseria, G. E.; Frisch, M. J. *Chem. Phys.* **1998**, *109*, 8128.
(59) Reed, A. E.; Weinhold, F. *J. Chem. Phys.* **1985**, *83*, 1736.
(60) Reed, A. E.; Curtiss, L. A.; Weinhold, F. *Chem. Rev.* **1988**, *88*, 899.
(61) Rotzinger, F. *J. Am. Chem. Soc.* **1996**, *118*, 6760.
(62) Casida, M. E.; Gutierrez, F.; Guan, J.; Gadea, F.-X.; Salahub, D.; Daudey, J.-P. *J. Chem. Phys.* **2000**, *113*, 7062.
(63) Casida, M. E. DFT2003 conference, Bruxelles, oral communication.